



Recent techniques of MRI in detection of pancreatic neoplasm

Essay submitted for partial fulfillment of Master Degree in diagnostic radiology

By

Michel Adel Mounir Gad

M.B., B.Ch

Ain Shams University

Supervised By

Prof. Dr. Suzan Bahig Ali

Professor of radiodiagnosis

Faculty of medicine

Ain Shams University

Dr. Remon Zaher Elia

Lecturer of radiodiagnosis

Faculty of medicine

Ain Shams University

Faculty of Medicine

Ain Shams University

2014



التقنيات الحديثة للرنين المغناطيسى فى تشخيص أورام البنكرياس

رسالة

توطئة للحصول على درجة الماجستير في الأشعة التشخيصية

مقدمة من

الطبيب / ميشيل عادل منير
بكالوريوس الطب والجراحة
جامعة عين شمس

تحت إشراف

أ.د. سوزان بهيج على

أستاذ الأشعة التشخيصية
كلية الطب
جامعة عين شمس

د. ريمون زاهر ايليا

مدرس الأشعة التشخيصية
كلية الطب
جامعة عين شمس

كلية الطب
جامعة عين شمس

2014

Recent techniques of MRI in detection of pancreatic neoplasm

CONTENTS	PAGE
• Acknowledgement	2
• List of abbreviations, figures and tables	3
• Introduction and Aim of work	9
• Chapter 1: Normal anatomy of the pancreas.	12
• Chapter 2: Pathology of pancreatic neoplasm.	31
• Chapter 3: Technique.	48
• Chapter 4: MRI appearance of pancreatic neoplasm.	74
• Summary and conclusion	101
• References	105
• Arabic summary	112

ACKNOWLEDGMENTS

I wish to express my great indebtedness and deep gratitude to **Dr. Suzan Bahig Ali**, Professor of Diagnostic Radiology, Faculty of Medicine, Ain Shams University for accepting the idea of this work, her kind assistance and efforts, which helped me in accomplishing this essay.

I also extend my thanks and appreciation to **Dr. Remon Zaher Elia**, Lecturer of Radiology, Faculty of Medicine, Ain Shams University for his invaluable guidance and great help in supervising this work. No words can express my feelings, respect and gratitude to him as regards his continuous encouragement and constructive criticism given to me at every stage of this work.

Words cannot express my feelings of gratitude towards my father, my mother, my brother, my future wife and all my friends for their unconditional love and support during the preparation of this work.

LIST OF ABBREVIATIONS

ADC	Apparent diffusion coefficient
AST	aspartate aminotransferase,
b-FFE	Balanced Fast Field Echo
CBD	common bile duct
CHESS	chemical shift selection
cho	Choline
CNR	contrast-to-noise ratio
cr	Creatine
CT	Computed Tomography
DCE	Dynamic contrast enhanced
DWI	Diffusion Weighted Images
eGFR	estimated glomerular filtration rate
ERCP	Endoscopic retrograde cholangiopancreatography
FFE	fast-field echo
FRFSE	fast recovery fast spin-echo
FWHM	Full- wave at half maximum
GE	Gradient Echo
GRE	Gradient Echo
HASTE	Half Fourier Acquired Single Shot Turbo Spin Echo
IPMN	Intraductal Papillary Mucinous Neoplasm
IR	Inversion recovery
LAVA	liver acquisition with volume acceleration
LDH	lactic dehydrogenase
MCN	Mucinous Cystic Neoplasm
MDCT	Multi-detector computed tomography
MEN	Multiple endocrine neoplasm
MIP	Maximum Intensity Projection
MPD	main pancreatic duct
MPR	Multiplanar reconstruction
MRA	Magnetic resonance angiogram

MRCP	Magnetic Resonance cholangiopancreatography
MRI	Magnetic Resonance Imaging
MRS	Magnetic Resonance Spectroscopy
MVD	microvascular density
NET	Neuroendocrine tumors
OC	one compartement
PACE	prospective acquisition correction encoding
PTC	percutaneous transhepatic cholangiogram
SAR	Specefic absorption rate
SAR	specific absorption rate
S-MRCP	Secretin-enhanced MR cholangiopancreatography
SNR	Signal to noise ratio
SPACE	sampling perfection with application optimized contrasts using different flip-angle evolutions
SPAIR	spectral adiabatic inversion recovery
SSFP	Steady State Free Precession
SSFSE	Single Shot Fast Spin Echo
SSh	Single Shot Short Half Fourier
STIR	Short time inversion recovery
T	Tesla
TC	two compartements
TE	Time of echo
THRIVE	T1-weighted high-resolution isotropic volume examination
TR	Time or repetition
True FISP	True Fast Imaging With Steady State Free Precession
TSE	turbo spin-echo
VIBE	volume interpolated breath-hold F-GRE
WBC	white blood count,
WIs	weighted images

LIST OF FIGUERS

Figure 1	Relations of the pancreas	13
Figure 2	Venous drainage of the pancreas	14
Figure 3	Variations in the ductal anatomy of the pancreas	16
Figure 4	Posterior relations of the pancreas.	19
Figure 5	Arterial supply of the pancreas.	23
Figure 6	Normal high signal intensity of the pancreatic parenchyma on this T1-weighted image.	26
Figure 7	post contrast T1W fat-saturated images of the pancreas	27
Figure 8	MR imaging shows the usual low signal intensity on this T2-weighted image	28
Figure 9	Normal coronal A) axial B) MRCP renderings and corresponding diagrams (C–D).	30
Figure 10	Histological features of the tumor (adenocarcinoma)	34
Figure 11	Serous cystadenoma	38
Figure 12	Pancreatic mucinous cystadenoma	39
Figure 13	Intraductal papillary mucinous neoplasm.	40
Figure 14	Gastrinoma in a patient with the Zollinger-Ellison syndrome	44
Figure 15	Intraductal papillary mucinous neoplasm, status post-Whipple operation. (A) Coronal MRCP image (B) Same patient after ingestion of negative oral contrast.	52
Figure 16	Acute pancreatitis (A) Axial T2weighted image. (B) Axial T1-weighted opposed-phase image	53
Figure 17	(A) Axial CT image. In-phase (B) and opposed-phase (C) images of 3-dimensional T1-weighted fat-only image (D).	54
Figure 18	(A) Axial SSFSE T2-weighted image. (B) Coronal MRCP image on the same study.	56
Figure 19	Navigator monitoring of respiratory motion.	58
Figure 20	Two-dimensional MRCP image in a 55-year-old man	59

	with right upper-quadrant pain.	
Figure 21	74-year-old woman with cystic pancreatic lesions.	60
Figure 22	47-year-old man with abdominal pain evaluated with MRCP.	62
Figure 23	48-year-old woman with chronic pancreatitis. (A) Conventional MRCP (B) Postsecretin MRCP (C) ERCP.	63
Figure 24	52-year-old woman with suspected chronic pancreatitis.	64
Figure 25	(A) Presecretin MRCP (B) 8 minutes after intravenous secretin injection.	65
Figure 26	MRS of normal pancreas.	69
Figure 27	The location image of Fig. 26 in T1WI.	70
Figure 28	Stage IA pancreatic cancer.	74
Figure 29	Stage IB pancreatic head cancer.	76
Figure 30	T4 pancreatic cancer, signs of non-resectability.	78
Figure 31	Serous cystadenoma.	79
Figure 32	Mucinous cystic neoplasms.	80
Figure 33	Cholangio-magnetic resonance image.	81
Figure 34	29-year-old woman with pancreatoblastoma.	82
Figure 35	Small insulinomas(a). After contrast administration, ring-like enhancement is characteristic (b)	83
Figure 36	Solid pseudopapillary tumor.	86
Figure 37	Abdominal MRI image, axial post contrast T1 with fat suppression.	87
Figure 38	Metastases to the pancreas.	88
Figure 39	Coronal thick slab MRCP shows the classical ‘double duct’ sign in a patient with carcinoma at the head of pancreas	89
Figure 40	Coronal MIP reformat shows intrahepatic bile duct dilatation and a grossly dilated CBD	90
Figure 41	Coronal MIP reformat shows a small multi-septated cystic lesion (arrow) arising in the uncinate process of	91

	the pancreas.	
Figure 42	Type 1 pancreatic adenocarcinoma in a 79-year-old woman. Lesion shows clear hyperintensity on axial DW image.	92
Figure 43	Type 2 pancreatic adenocarcinoma In a 74-year-old man. Lesion is hyperintense on axial DW image.	93
Figure 44	ADCs of type 1 pancreatic adenocarcinoma with clear hyperintensity	94
Figure 45	MRS of normal pancreas	95
Figure 46	MRS of pancreatic cancer.	95
Figure 47	The location image of Fig. 46 in T1WI	96
Figure 48	The ROC curve of diagnosing pancreatic cancer	96
Figure 49	Normal individual where regions of interest are over non-tumor (purple) and reference (pink), abdominal aorta (red)	99
Figure 50	Case of pancreatic cancer	100
Figure 51	Case of pancreatic metastasis from hypernephroma	100

LIST OF TABLES

Table 1	Classification of pancreatic tumors.	31
Table 2	TNM categories in pancreatic cancer.	35
Table 3	Differential of cystic pancreatic lesions.	36
Table 4	Parameters of pancreatic imaging on 1.5 T MRI imaging scanners	50
Table 5	Parameters of pancreatic imaging on 3.0 T MRI imaging scanners.	51
Table 6	T1-weighted Turbo Field-Echo DCE MR Imaging Parameters	72
Table 7	SI Curve Pattern, DCE MR Quantitative Parameters, and Histopathologic Parameters	101

INTRODUCTION

The pancreas is a tongue shaped organ, approximately 12 -15 cm in length, that lies within the anterior pararenal compartment of the retroperitoneum. (*Brant et al, 2012*)

Pancreatic cancer is the fifth leading cause of cancer related death in both men and women and is responsible for 5% of all cancer-related deaths in the United States. (*Yoon et al, 2010*)

The most recent classification divides pancreatic disorders into primary tumors including epithelial endocrine and exocrine as well as non-epithelial neoplasms, secondary neoplasms, and tumor-like conditions (*Kloppel et al, 2004*).

Compared with CT, MRI has the advantage of being able to detect cystic changes within pancreatic masses and to provide more accurate morphological detail on these changes. (*Yoon et al, 2010*).

MRI plays a triple role in the evaluation of the pancreas: Diagnosis, staging, and detection of complications. The role of MRI has increased, especially in imaging patients with suspected pancreatic neoplasms (*Olivia et al, 2006*).

To evaluate pancreatic lesions accurately, the use of multiple pulse sequences that provide complementary information is required, and, in

INTRODUCTION

general, a combination of T1-weighted (T1W) and T2-weighted (T2W) sequences is obtained. (*Olivia et al,2006*).

The intravenous (IV) administration of an extracellular contrast agent (gadolinium chelate) is a useful adjunct in the MRI examination of the pancreas. It can help differentiate hypervascular pancreatic masses that may simulate cystic lesions on noncontrast scans. (*Olivia et al,2006*).

MR Spectroscopy has been used as a tool in the differentiation of pancreatic cancer from chronic focal pancreatitis and in the detection of hepatopancreaticobiliary cancer. Pancreatic cancer and chronic focal pancreatitis are difficult to discriminate initially because of their similar clinical and radiologic features at presentation. (*Shah et al, 2006*).

Diffusion weighted (DW) imaging allows detection of pancreatic adenocarcinomas with high sensitivity and specificity. Previous studies have found that pancreatic adenocarcinoma appears hyperintense compared with the rest of the gland on DW images, and DW imaging might have potential to become the imaging modality of choice for screening patients at high risk for pancreatic adenocarcinoma. (*Fukukura et al, 2012*).

In oncologic studies, dynamic contrast agent–enhanced MR imaging may be performed to provide information concerning tumor microvasculature, and it has been used as a biomarker for tumor response to treatment. (*Bali et al, 2011*)

INTRODUCTION

AIM OF WORK

The aim of this study is to highlight the role of the new techniques of MRI in evaluation pancreatic neoplasm.

ANATOMY OF THE PANCREAS

The pancreas is a tongue shaped organ, approximately 12 -15 cm in length that lies within the anterior pararenal compartment of the retroperitoneum. It is composed of four parts (head, body, neck and tail).

(Brant et al., 2012)

PARTS

Head:

The head of the pancreas lies to the right of the midline, anterior and to the right side of the vertebral column, within the curve of the duodenum. Superiorly it lies adjacent to the first part of the duodenum. The inferior border lies superior to the third part of the duodenum and is continuous with the uncinate process. Close to the midline, the head is continuous with the neck. The boundary between head and neck is often marked anteriorly by a groove for the gastroduodenal artery and posteriorly by a similar but deeper deep groove that contains the union of the superior mesenteric and splenic veins as they form the portal vein. *(Standering et al., 2008)*

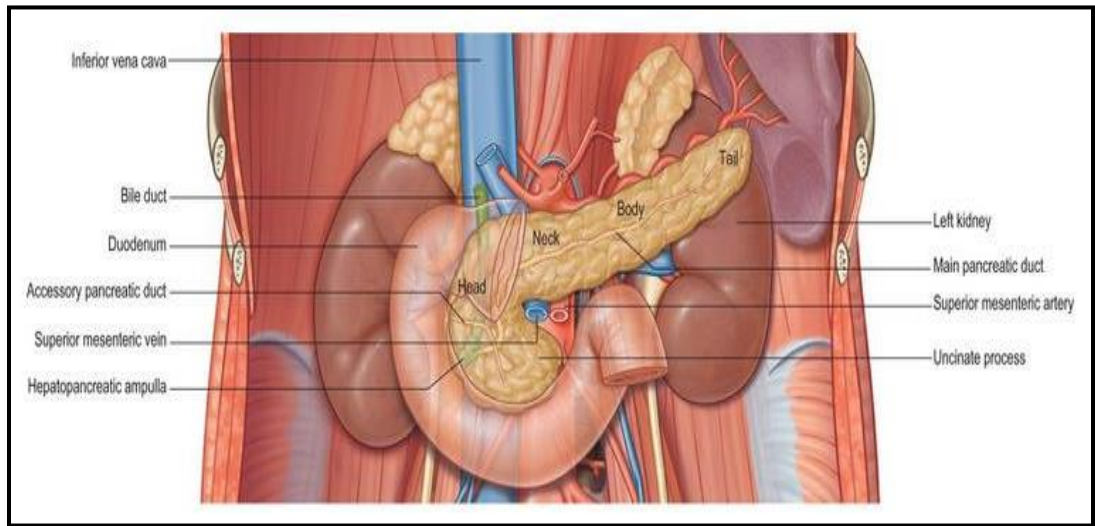


Fig.1 relations of the pancreas (*Standerling et al., 2008*)

Neck:

The neck of the pancreas is approximately 2 cm wide and links the head and body. It is often the most anterior portion of the gland and is defined as the portion of the pancreas that lies anterior to the portal vein, which is closely related to the upper posterior surface (see **Fig. 2**). The lower part of the neck lies anterior to the superior mesenteric vein just before the formation of the portal vein. (*Standerling et al., 2008*)